Role of solar activity in many-year variability of photochemical components of the lower troposphere

M.Yu. Arshinov, B.D. Belan, V.K. Kovalevskii, T.M. Rasskazchikova, T.K. Sklyadneva, and G.N. Tolmachev

Institute of Atmospheric Optics, Siberian Branch of the Russian Academy of Sciences, Tomsk

Received September 16, 2002

We have found earlier that air components of photochemical origin vary with the 11-year periodicity, and concentrations of ozone and aerosol lag behind the solar activity by 2–3 years. To find the reasons for this phenomenon, we have analyzed the ozone mechanism, as well as consequences of variations in the UV radiation influx. The analysis revealed some intermediate mechanism, which is likely caused by the interaction of the increasing UV irradiation with plants. At the beginning of UV irradiation increase, some inhibition of plant's growth is noticed. After 1–2-year adaptation period, some increase in plant's productivity appears leading to extra emissions of ozone- and aerosol-forming substances into the atmosphere. This hypothesis was checked using the normalized vegetation index and gave good results. Based on the regularities revealed, we make a prognosis of variations of the ozone and aerosol concentrations from 2003 to 2008.

Introduction

Many-year monitoring of air composition conducted by us from the early 1980s has revealed a periodicity in variations of the annual mean aerosol and ozone concentration close to 11 years. According to the present-day ideas, this periodicity is a reflection of solar activity. However, the mechanism of a signal transmission from the Sun to the lower troposphere is still unclear. Therefore, in this paper we analyze solar-terrestrial relations available in literature and compare them with the results of our measurements.

As far back as in ancient time people noticed that many processes on the Earth's surface depend on the Sun. Being a giant plasma sphere supplying energy to all terrestrial processes, the Sun is subject to internal dynamic processes,[1,2] which are called solar activity.

Chizhevskii was one of the first scientists, who comprehensively studied manifestations of the solar activity in physical, chemical, biological, and even social processes.[3] He has found a statistical relationship between the intensity of the solar activity measured in Wolf numbers[4] and changes in climate, water level of closed lakes, plant blooming period, plant growth rate, crop capacity, epidemic and pandemic periods, spikes in human cardio-vascular morbidity, social cataclysms, etc.

Further studies by many scientists complemented and expanded the data on the solar–terrestrial relations and made clear their mechanisms in the upper atmosphere. These relations are generalized in Ref. 5. The most important among them are the following:

1) Relations "solar activity – biological processes" are controlled by weather phenomena, and their effect is not reduced to the effect of traditional weather factors, such as temperature, partial oxygen pressure, etc., but consists in phytotron.

2) Heliobiological relations manifest themselves separately under different effects of the solar activity, such as chromospheric flares followed by magnetic storms, alternation of the interplanetary magnetic field sign, etc. Individual perturbations for a particular object interfere in a complex way and can intensify or attenuate each other. Every perturbation source has a characteristic time scale.

3) Effects similar to heliobiological ones take place in physico-chemical processes as well. Therefore, the effect of the solar activity is a universal natural phenomenon.

Based on the data of Refs. 4 and 5, Table 1 summarizes manifestations of the solar activity in different forms of geophysical fields.

It follows from Table 1 that the known energetically significant geophysical fields are subject to the effect of the solar activity of ultra-low-intensity. Those having the factor of 10–100 are either energetically weak for the natural medium or efficient only in the upper atmospheric layers and, therefore, incapable of affecting objects directly in the surface atmosphere.

At the same time, no obvious mechanisms of the signal transfer from the Sun to the fields listed follow from Table 1. Therefore, may be, there appear assumptions in the scientific literature on the biological action of the vector potential of the electromagnetic field, effect of a "sea" of cold neutrino, the presence of a "microlence" gas, and "torsion fields," etc.[4] However, these assumptions have no scientific basis yet.

0235-6880/02/12 958-15 $02.00

Table 1

Physical factor	Effect	Measurement amplitude
Weather parameters	Latitude and region dependence. Alternation of atmospheric circulation types. Interference	Synoptic scale
Concentration of aeroions	Interference with weather and regional conditions	Factor 2
Atmospheric radioactivity (Rn^{222})	Increase during magnetic storms (except for sea basins)	Factor 3
Electric field of the atmosphere	Latitude dependence. Solar flares. 11-year cycle	Factor 1.5–2
Geomagnetic field (index A_p)	Latitude dependence. All forms of solar activity	Factor 10
Atmospherics (f < 100 kHz)	–«–	Factor 100
Cosmic rays	–«–	Few percent
UV-B radiation	27-day period. 11-year cycle	2–4%
Atmospheric intrasound	Magnetic activity	Factor 2
Geomagnetic field strength	All forms of solar activity	No more than 1%

Rather comprehensive consideration of main channels of energy transfer from the Sun to the Earth can be found in Refs. 6–9. In accordance with Ref. 6, we begin with consideration of general pattern of interaction of solar and cosmic rays with the interplanetary space, Earth's magnetosphere, ionosphere, neutral atmosphere, and surface. Figure 1 represents the structure of relations between the most important channels of energy income from the Sun and those atmospheric layers, which can be accessed to radiation of some or other wavelength.

It is seen from Fig. 1 that the most part of the solar energy is spent already in the upper atmosphere. The troposphere is mostly accessible to the visible solar rays, strongly attenuated UV rays, and insignificant amount of flare protons and cosmic rays. Likely, the mechanism of solar energy transfer to the Earth should be sought in the channels, which are most energetically justified.

A large number of different indices is commonly used to characterize the solar activity, and the main of them, according to Ref. 5, are presented in Table 2.

In addition to the indices listed in Table 2, some scientists have introduced combined indices. Their characteristics can be found in Ref. 10.

No clear mechanism of transporting the solar energy to the lower tropospheric layers can be revealed from the above general schemes (Tables 1 and 2, Fig. 1). Therefore, we turn to the papers considering individual aspects of the solar–terrestrial relations.

Condensation cluster mechanism

The cluster mechanism is determined by the corpuscular radiation penetrating deep into the atmosphere and partly reaching the Earth's surface.[6,11] The flux of galactic cosmic rays continuously coming to the atmosphere from space looses the bulk of its energy in the lower stratosphere and upper troposphere. According to the balloon-borne measurements of the ion generation rates, the maximal ion concentration is at the altitudes of 12–20 km. Air ionization in the upper troposphere favors the formation of numerous condensation nuclei, which serve to active sublimation of water vapor at low temperatures (from – 40 to – 50°C) and to cirrus formation. According to the data of Ref. 11, in the period of increased income of cosmic rays, the concentration of aerosol particles with the radius from 0.1 to 1 μm increases 2–4 times.

Since the intensity of galactic cosmic rays is modulated by the solar activity (the modulation depth achieves 30%), all the periodicities characteristic of its magnetic component are imposed on meteorological processes. Besides galactic cosmic rays, solar cosmic rays also take part in realization of the condensation cluster mechanism. According to Ref. 12, the effect of solar cosmic rays on microphysical and optical parameters of the upper troposphere can be distinguished even at moderate solar flares.

The condensation mechanism also takes part in formation of the effect of solar activity variations through low-speed solar wind flows.[13] In addition to the direct effect on the Earth's magnetosphere, electric charges continuously drift into the ionosphere due to the solar wind and thus change its potential. Increased vertical electrical currents intensify microphysical processes in clouds. According to the conclusions drawn in Ref. 13, the nucleation rate and the rate of initial growth of ice crystals strongly depend on the rate of increase of the number of charges on supercooled droplets. The heat released at stimulated freezing of supercooled droplets should intensify vertical motions in the atmosphere and affect the global atmospheric circulation, whose variations may show themselves as long-term effects in the 11-year solar activity cycle.

Thus, the condensation mechanism leads to decrease in the solar radiation influx. According to the data of Ref. 14, the changes in the solar radiation influx with variations of galactic cosmic rays make ± 4–6%. This can play the role of the power source of perturbations in the large-scale atmospheric circulation that are observed in the 11-year solar activity cycle.

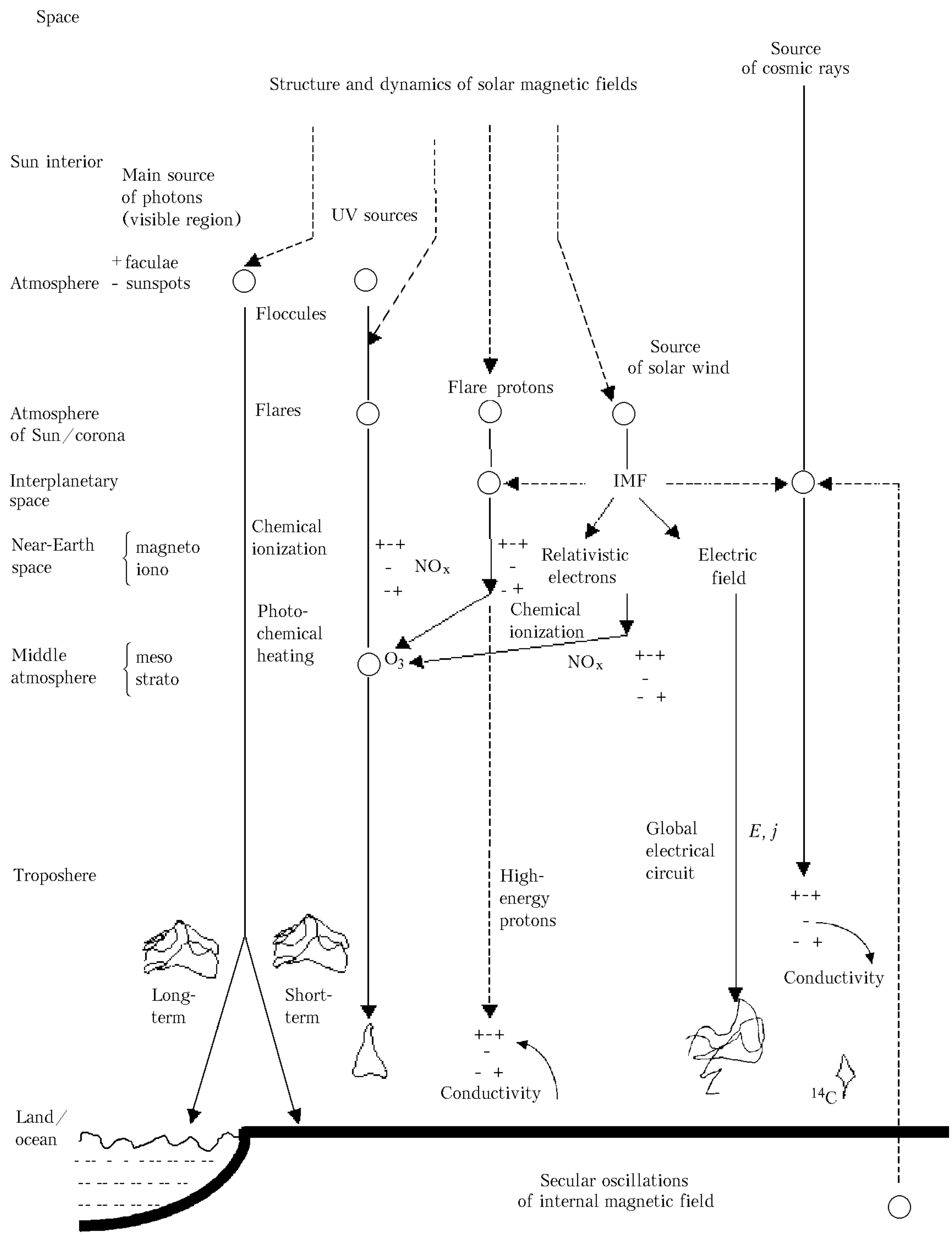

Fig. 1. Schematic representation of energy income from the Sun and from space through different channels illustrating their continuous or sporadic variability (wave or stepwise-wave designations) and atmospheric layers subject to the effect of this variability.[3] Some designations: E and j are, respectively, the electric field strength and current in the atmospheric electrical circuit; IMF is interplanetary magnetic field; NO_x are nitrogen oxides generated under the effect of solar protons; ^{14}C is radioactive carbon isotope formed under the effect of galactic cosmic particles; O_3 is ozone formed under the effect of solar UV radiation with $\lambda < 242$ nm; flares and floccules are solar photospheric and chromospheric magnetic structures having increased brightness.

Table 2

Index and accepted designations	Initial material for formation of an index. Type of observations according to international classification	Physical meaning and peculiarities of the index	Time interval	Method of calculation	Variability limits. Series length	Notes
1	2	3	4	5	6	7
Wolf numbers. Relative numbers of sunspots R, W	Sun image in the white light (photoheliograms). $R = K(10g + f)$, g is the number of sunspot groups; f is the total number of sunspots; K is fitted for every telescope	Physical meaning is unclear. This index attaches much importance to individual small sunspots. Monthly mean R characterizes the number of spots on the Sun surface	The index is determined every day. Monthly mean value (or, better, the value smoothed over several months) has a meaning	The index is determined by many observatories. Data are available in WDC-B2	From 0–3 to 150–250. Measured since 1749	R_Z is Zurich value; R_1 or $-R_0$ is American value
Total area of sunspots S	Photoheliograms $S = \sum_i S_i$ – summation over all spots; S_i is spot area	This index roughly reflects the magnetic flux in spot groups. Overestimates the role of large spots with developed penumbra	Monthly mean values are used (determined daily)	The index is determined by many observatories. Data are available in WDC-B2	From 0 to several thousands m.f.a. 85% groups are less than 250 m.f.a., but there are groups up to $2\cdot10^3$ m.f.a. Measured since 1874	M.f.a. is the millionth fraction of the area of the Sun hemisphere
Solar radio emission F_λ (most often at 2800 MHz or 10.7 cm)	Solar radiation records. Measured in solar flux units (s.f.u.) 10^{22} W/m^2. Sometimes observed F_λ is recalculated to F_λ at the distance of 1 a.u. from the Sun i.e. to F_a	This index characterizes temperature and density variations all over the area of all active regions of the visible disk (not only in sunspots)	Temporal variations well correlate with variations of R and S. This index may be a convenient characteristic of daily activity	Measured by many radio-astronomical institutions, but the spread between absolute values obtained by different observatories is very wide	$F_{10.7}$ varies within 50–300 s.f.u.; daily mean values or values for a certain time (local noon) are usually presented	Daily variability by a three-grade system is sometimes presented. This index is determined regardless of weather and can serve a measure of soft X-ray radiation of the Sun (1–100 Å)
Calcium plage daily index $I_{Ca(II)}$	Calcium spectroheliograms $I_{Ca} = \frac{1}{1000}\sum_i I_i A_i \cos\theta_i \cos\varphi_i$, θ_i is the angular distance from the central meridian; φ_i is heliolatitude; I_i is brightness by 5-grade scale; A_i is plage area in m.f.a.	The index accounts for areas and brightness of all active regions; it is sensitive to variations of magnetic field strength. The role of inactive large floccule fields is overestimated	Daily mean values are used	Calculated in Ionosphere Laboratory of the University of Pennsylvania, USA	0–100 Since 1958	Total area of calcium floccules for every day is presented
Daily index of flare activity I_f	H_α are flare patrol films, $I_f = 0.76/T^* \sum A_\alpha^2$, A_α is uncorrected area in 10^{-6} fractions of the solar disk area; T^* is the effective patrol time, min	Gives an idea about energy released in nonstationary processes	Daily characteristic. Flare effects are studied by superposed epoch method	Calculated by WDC, A_α is obtained from WDC chromospheric patrol data	0–500. Since 1969	Strongly depends on the weather. There are no predictions for I_f. Daily predictions of flares are made in different prediction centers

Table 2 (continued)

1	2	3	4	5	6	7
Direction (sign) of interplanetary magnetic field	Records of the Earth's magnetic field at Vostok and Tule polar observatories	Geoefficiency of solar activity sometimes depends on the IMF direction and on intersection of IMF sector boundaries by the Earth (i.e., on IMF sign alternation). Sign+ corresponds to IMF direction from the Sun to the Earth	Characteristic of IMF direction during observations	Determined from the data of polar stations in ISMIRAN by the Mansurov technique and Svaalgard (Boulder, BSA). Accurate values of IMP sign and strength are determined with the help of satellites	Since 1926	The probability of correct estimation of IMF sign by the ground-based data is 80–90%

Ozone mechanism of assimilation and filtering of the solar radiation

The ozone layer located between the mesosphere and the stratosphere plays an important role in formation of the damping-connecting mechanism between systematic and spontaneous factors of the solar activity and weather-climate changes.

The ozone mechanism of solar activity is determined by a complex system of physical-chemical processes occurring under the simultaneous, but diverse impact of all solar factors on the illuminated side of the Earth and only of a part of them on the night side.[6] The most significant effect on the ozone layer state is due to the UV solar radiation (λ < 242 nm) and cosmic rays of the galactic and solar origin. The total ozone content (TOC) can vary in different ways under the effect of different components of solar radiation. Thus, the increase in the radiation influx at λ < 310 nm leads to the TOC increase and vice versa.[15] Bursts of solar cosmic rays should result in formation of excessive nitrogen oxide in the middle atmosphere,[16] which, in its turn, modifies the mechanism of ozone generation and sink in the stratosphere.[17]

Two comprehensive recent reviews[18,19] devoted to analysis of the ozone and TOC dynamics reveal many-year trends of these components in the atmosphere. At the same time, the attempts to find a continuous stable relation between TOC and solar activity failed.[6] In some decades, the correlation between their series is positive, while in the others the cross-correlation with a 3–4-year shift is positive, and for the period of 1933–1959 a negative correlation was observed for stations in the Northern Hemisphere. Different factors possibly play the decisive role in the ozonosphere dynamics in different 11-year cycles of the solar activity. Only in Ref. 20, no statistically significant changes in TOC were found for 19 proton events and 21 cases of decrease in galactic cosmic rays. This result is quite natural, since TOC is determined by two mechanisms: ozone generation near the 50-km level and its accumulation in the layer below 30 km, where it is a conservative pollutant.[21] Charged particles possibly caused some short-term effect at the altitude of 50 km, but its contribution to TOC was, most likely, insignificant.

Nevertheless, since the long-term variations of the ozone concentration in the stratosphere took place (what is almost equivalent to TOC variations[15–19]), they should, keeping in mind the high activity of ozone, affect other atmospheric processes. We can distinguish two possible variants, each connected with absorption of the solar UV radiation by ozone.

The decrease or increase of the ozone concentration in the stratosphere leads to the decrease or increase of the air temperature at the corresponding altitudes. According to the results of Ref. 19, the TOC trend in 1979–1994, caused mostly by the ozone depletion in the lower stratosphere, was accompanied by the temperature decrease trend at the same altitudes (about 0.6°C for 10 years).

A change of the air temperature may lead to the increase or decrease in the pressure gradient and, correspondingly, disturb the air circulation. This hypothesis was checked using the ICM RAS global circulation model.[22] Qualitatively, the model data on variations of the ozone concentration are very similar to the actually observed pressure difference, but their values are roughly 1.5 times lower than the observed ones.

According to calculations,[19] the decrease in the content of the stratospheric ozone starting from the 1980s can compensate for about 30% of the greenhouse global climate warming.

The TOC variations should also tell upon the UV radiation influx into the troposphere, causing various effects, which will be considered below.

The first published data on the response of the UV radiation to the TOC decrease in 1992–1993 gave contradictory results. Thus, according to Ref. 23, the decrease in the TOC level was not accompanied by the increase in the UV radiation influx. The results of Ref. 24 indicate that the reverse is true: the increase of the UV radiation was observed in northern mid-latitudes after the decrease in the ozone level in 1992–1993.

In the following years, many researchers studied this problem and obtained interesting results. It is worth considering them in more detail.

In Ref. 25, it was found from measurements in the Antarctic for two periods of 1979–1980 and 1990–1994, when TOC decreased, that the increase in the UV radiation in the band of 295–310 nm achieved 50–65%. In Ref. 26, it was revealed that the long-term variations of the UV-B solar radiation due to the ozone change by 4.5% for 10 years were 10% at λ = 305 nm, and the two-year TOC change by 8% led to the change by 21% in the radiation at λ = 295 nm.

The investigations conducted within the World Climate Research Programme[27] showed that during almost seven-year observation period no UV radiation trends were observed in Loder. This result is quite natural, because no TOC trends were observed in that period.

The data of Ref. 28 obtained in Scotland are indicative of the UV radiation growth by 35% for 1986–1992, when the TOC decreased by 10%. The UV-B radiation growth from 3 to 10% a year at the decreasing TOC was observed at Point Barrow, Alaska.[29]

The recent observations in mountainous regions[30] have shown that as the height increases, the UV radiation grows markedly due to the decrease of the atmospheric depth and change in the optical properties of the atmosphere. According to the findings of Ref. 31, this growth in the Swiss Alps achieved 9–23% per 1 km. According to the Cabrera data,[32] in Chili the vertical gradient of the UV-B radiation was equal to 4–10% per 1 km, and near Santiago it increased up to 40% per 1 km. Thus, the significant part of the UV radiation is spent in the lower 1-km layer.

The observed changes in the UV-B radiation are summarized in Ref. 19:

1. A considerable increase in the UV radiation due to the ozone hole in the Southern Hemisphere was found. The results of numerical simulation and measurements agree well.

2. Measurements of the UV radiation at clear sky in the mid-latitudes of the Southern Hemisphere gave higher values than at the corresponding points of the Northern Hemisphere. This fact agrees with the differences in the TOC decrease and the Sun–Earth distance in the corresponding seasons.

Measurements in 1992–1993 in the middle and high latitudes of the Northern Hemisphere revealed local increases in the UV-B radiation. Spectral signatures of the radiation increase point to the effect of the abnormally low TOC level in these years, rather than the consequence of cloud cover variability or tropospheric pollution.

Calculations show that the increase of the UV-B radiation at clear sky in the period 1979–1993 due to TOC variations is maximal at short waves and in high latitudes.

Scattering of the UV radiation by the aerosol produced at the Mt. Pinatubo eruption did not affect markedly the total level of the near-surface UV radiation.[33]

The increase of the UV radiation can be both positive and negative. This issue will be discussed below. In the following section, we consider one more possible mechanism of signal transmission from the Sun to the Earth.

Direct effect of changes in the extraterrestrial spectral distribution of the solar radiation

Under ordinary conditions (absence of any solar events), the solar UV radiation influx is almost continuous and makes up 5–7% of the integral influx.[34,35] Although the UV radiation influx depends on the weather conditions, it, on the whole, is proportional to the integral radiation influx. This allowed Kruchenitskii et al.[36] to propose the approximating equation to calculate the diurnal exposition of the Earth's surface to the UV-B radiation accurate to about 15%:

$$Q = 6.13(1 + 0.18R) \times$$
$$\times \int_{t_1}^{t_2} dt \, \{\exp[-K(b)x(t)]\,[\exp(0.8 \sin V - 1)]^{2.16}\}.$$

Here Q is the diurnal exposition of the Earth's surface to the UV-B radiation, in W·h/m^2; $R = 1$ in the presence of the snow cover and $R = 0$ in its absence; V is the Sun elevation angle at the time t;

$$K(b) = 0.0388 + 0.000532\,\{1 + \tanh[2.3(b - 8.28)]\} +$$
$$+ 0.0002\,[1 + \tanh(b - 5.56)] +$$
$$+ 0.000033\,\{1 + \tanh[3.6(b - 1.5)]\};$$

$b(t)$ is the cloud amount; $x(t)$ is the total ozone content (D.u.); t_1 and t_2 are the sunrise and sunset times, respectively.

Development of absolute satellite radiometry[37–39] provided climatologists with many-year series of data on diurnal variations of the integral solar constant, its 27-day periodicity, and 11-year cycle of the solar activity. The main results obtained from the data processing are summarized in Ref. 7. It turned out that the mean annual value of the integral solar constant varied within 0.1% during the 11-year solar activity cycle and the 27-day variations due to the Sun rotation did not exceed 0.3%. Consequently, many-year variations of the solar radiation influx are insignificant. Nevertheless, accepting these results, Sklyarov et al.[40] note that even these minor variations are synchronized with the 11-year solar cycles.

The data on the small variability of the integral solar constant have led Kondratyev and Nikol'skii[7] to the conclusion about the need of considering spectral variations of the extraterrestrial solar radiation. Their analysis of observations have shown that as the active region crosses the central solar meridian and at concourse of solar-related circumstances, the Earth is illuminated by radiation with the maximum intensity nearby 410 nm and the anomalous spectral behavior. The largest increase in the radiation intensity was found in the region of 330–430 nm. In this case, the excessive radiation is generated by a very small part (10^{-7}) of the solar disk surface.

According to Ref. 2, the contributions of dark sunspots and bright faculae to the sun brightness are mutually compensated (accurate to 10%). The many-year behavior is indicative of 11-year oscillations of the global sun brightness, which are not strictly synchronous with the solar activity cycles. Thus, the behavior of the brightness at the growth phase of the 11-year sunspot cycle lagged 1 year behind the behavior of the Wolf numbers, while at the drop phase it, on the contrary, was 1.75 year ahead the behavior of the Wolf numbers.

Thus, some fluctuations in the spectral composition of the radiation exist against the background of the relatively constant radiation influx from the Sun to the Earth.

Possible consequences from variations in the UV radiation influx to the troposphere

It follows from the above-said that the extra amount of the UV radiation can come into the troposphere due to the solar activity. In this section, without dwelling on the mechanism responsible for the variations, we consider their possible consequences for the atmosphere and biosphere.

In our opinion, two issues can be analyzed. The first one is that the UV radiation is the prime cause of photochemical processes leading to generation of ozone and fine aerosol.[41] Consequently, the chemical composition of air varies. The second issue, more poorly studied in spite of numerous publications, is the response of the biosphere to variations in the UV irradiance. Here we speak about plants, which produce the huge amount of substances for ozone and aerosol generation, what finally results in variations of the air chemical composition as well.

First, let us discuss variations in the intensity of photochemical processes.

According to Refs. 42 and 43, photochemical processes in the troposphere begin with photolysis of available ozone through one of the following reactions:

$$O_3 + h\nu \rightarrow O_2 + O(^3P), \quad 320 < \lambda < 400 \text{ nm},$$
$$O_3 + h\nu \rightarrow O_2 + O(^1D), \quad \lambda < 320 \text{ nm},$$

or other substances, usually, of anthropogenic origin:

$$NO_2 + h\nu \rightarrow NO + O(^1P), \quad \lambda < 400 \text{ nm};$$
$$CH_2O + h\nu \rightarrow CHO + H, \quad \lambda < 335 \text{ nm};$$
$$CH_2O + h\nu \rightarrow CO + H_2, \quad \lambda < 360 \text{ nm}.$$

About 90% of oxygen atoms $O(^1D)$ formed by the second reaction, interacting with air molecules, transit into the ground state $O(^3P)$ and repeatedly transform into ozone:

$$O(^1D) + N_2, O_2 \rightarrow O(^3P) + N_2, O_2,$$
$$O(^3P) + O_2 + M \rightarrow O_3 + M.$$

The residual 10% of $O(^1D)$ under normal conditions react with the water vapor with formation of hydroxyl:

$$O(^1D) + H_2O \rightarrow 2OH.$$

Besides, $O(^1D)$ can interact with nitrous oxide transforming it into rather reactive nitric oxide[44]:

$$N_2O + O(^1D) \rightarrow 2NO$$

and with methane and hydrogen with formation of hydroxyl:

$$CH_4 + O(^1D) \rightarrow CH_3 + OH;$$
$$H_2 + O(^1D) \rightarrow H + OH.$$

Further behavior of the air system depends on the concentration of minor atmospheric gases. In the absence of CO or hydrocarbons, the photochemical equilibrium between nitric oxides and ozone is established in the troposphere:

$$NO + O_3 \rightarrow NO_2 + O_2;$$
$$NO_2 + h\nu \rightarrow NO + O(^1P);$$
$$O + O_2 + M \rightarrow O_3 + M.$$

If nitric oxides, carbon oxide, or hydrocarbons are present in air, then the ozone generation begins by one of the schemes given below:

$CO+OH \rightarrow CO_2+M$;	$CH_4+OH \rightarrow CH_3+H_2O$;
$H+O_2+M \rightarrow HO_2+M$;	$CH_3+O_2+M \rightarrow CH_3O_2+M$;
$HO_2+NO \rightarrow NO_2+OH$;	$CH_3O_2+NO \rightarrow CH_3O+NO_2$;
$NO_2+h\nu \rightarrow NO+O$;	$HO_2+NO \rightarrow NO_2+OH$;
$O+O_2+M \rightarrow O_3+M$.	$2(NO_2+h\nu \rightarrow NO+O)$;
	$2(O+O_2+M \rightarrow O_3+M)$.
$CO+2O_2+h\nu \rightarrow CO_2+O_3$	$CH_4+4O_2+h\nu \rightarrow$ $\rightarrow CH_2O+H_2O+2O_3$

It can be seen from these schemes that photochemical processes can begin only in the presence of UV radiation quanta at $\lambda < 400$ nm. It is well-known that the solar radiation at $\lambda = 295–400$ nm reaches the lower tropospheric layers. Consequently, the initially needed photodissociation by the above reactions should take place.

The photodissociation rate of ozone molecules can be determined by the following equation[45]:

$$J = \int_{\lambda_1}^{\lambda_2} F_\lambda \sigma_\lambda \varphi_\lambda d\lambda,$$

where σ_λ is the absorption cross section at the wavelength λ for the ozone molecules; φ_λ is the quantum yield characterizing the probability of dissociation of a molecule after absorption of a light quantum with the wavelength λ.

The radiation flux F_λ determining the photodissociation rate at the level z is described by the equation

$$F_\lambda(z) = F_\lambda^0 \exp[-(\tau_{ab} + \tau_{sc})] + F_\lambda^P(z, A),$$

where F_λ^0 is the extraterrestrial solar radiation flux; τ_{ab} and τ_{sc} are the optical depths caused by radiation scattering and absorption along the direction of its propagation; F_λ^P is the radiation flux scattered by gases, aerosol, and the surface having the albedo A.

It follows from the last two equations that, all other conditions being the same, the higher F_λ^0, the higher the ozone photodissociation rate and the greater amount of ozone is produced in the photochemical processes.

In Refs. 46 and 47, the attempts were undertaken to estimate the increase in the dissociation rate at the actually observed variations of UV radiation at the varying solar activity. In Ref. 46 it was found that the UV growth by several percent can lead to increase in production of $O(^1D)$ and OH up to 50% under unpolluted conditions and up to 75% under polluted conditions. Similar result was reported in Ref. 47 as well.

The inverse behavior of TOC and tropospheric ozone near Tomsk was reported in Ref. 48. Because of the absence of measurements of UV radiation, a relative change of the photodissociation rate equivalent to the TOC variations was calculated and compared with variations of the near-surface ozone concentration. The difference between the calculated and experimental data was within 5%.

In Ref. 49, the photochemical model was used to calculate the effect of the total ozone variations on the tropospheric chemistry. It was shown that the TOC decrease from 320 to 270 D.u. and the corresponding increase of UV radiation led to the increase in photochemical activity and formation of radicals.

In Ref. 50, the photolysis rates for some atmospheric gases of photochemical origin were measured directly. The results obtained confirmed both the theoretical and empirical estimates.

And, finally, in Ref. 51 the attention was paid to the fact that the increase in the pollutant concentration near the ground in polluted regions compensated the increase of the UV-B radiation for the last 50–100 years. In such regions, it manifests itself above the boundary layer.

Thus, now we have both the calculated and experimental data confirming the role of the UV radiation in variations of the air composition.

Possible reaction of plants to variation of UV-B radiation in the troposphere

According to Ref. 52, plants and the World Ocean produce almost one-third of air constituents, which take part in photochemical processes. Plants and oceanic phytoplankton should response to changes in UV radiation influx, and this section is devoted to analysis of such processes. The biosphere is surprisingly resistant to external effects.[53] As was shown in Ref. 54, the Earth's biota obeys the well-known Le Chatelier principle: external perturbations distorting the state of the environment initiate biospheric processes compensating these perturbations.

The plant response to variations in the UV irradiance was considered in numerous publications.[34,35,55–58] Their main results can be generalized as follows.

The shortwave boundary of the spectrum for photosynthesis of green plants is $\lambda = 330$ nm. The shorter-wave ($\lambda < 330$ nm) UV radiation sharply inhibits photosynthesis.

One of the main problems arising when studying the effect of UV radiation on plants is to clarify whether this effect is stimulating or inhibiting. It was found experimentally that UV radiation at $\lambda < 295$ nm has a stable inhibiting effect. The effect of the UV-B radiation ($\lambda = 295$–320 nm) on plants depends on the dose: small (for a given plant) doses have a stimulating effect, while large doses inhibit the plant. The information about doses for various biological species can be found in Refs. 59–61. To estimate the threshold plant-hazardous dose of UV radiation, as well as to study the plant sensitivity to UV irradiation, 2500 plants of 19 species were irradiated by bactericide radiation with the wavelength of 253.7 nm (Ref. 34). This experiment showed that the threshold irradiation dose for different plant species varied in the ratio of 1:50. Its minimal value corresponded to the lethal dose for microorganisms.

It is important to emphasize that the UV-B radiation even in large doses is useful for mountain plants, while lowland plants are tolerant only to its small doses.

Besides, the UV-B radiation is intensely absorbed by protein, chlorophyll, and other substances, therefore its increase affects the vital activity of plants, what is supported by the available data.

The UV-A ($\lambda = 330$–400 nm) and UV-B ($\lambda = 295$–320 nm) radiation does not accelerate seed germination, but after germination the UV irradiation favors the growth of a strong and enduring plants. Vegetable and flower seeds irradiated by the UV radiation keep germinating capacity when stored in closed vessels for 10 years and only 5 years under standard conditions.

Thus, there is a good reason to believe that plants response to variation of UV radiation influx.

In the context of variations in the chemical composition of air, it is interesting to consider volatile organic compounds emitted by plants into the atmosphere. This issue was thoroughly considered in Ref. 62. The composition, rate, and volume of emission, as well as its dependence on the air temperature were determined for numerous plant species. The temperature dependence is especially important for our analysis, since the temperature of the surface air is proportional to the solar radiation influx.

In some papers, solar radiation was taken into account along with the air temperature. Thus, in Ref. 63, the emissions of isoprene and monoterpenes from 40 plant species were measured in the Mediterranean region in 1993–1997. The emission values correlated with the temperature and the photosynthetically active radiation. The measurements over boreal wetlands in Scandinavia[64] also have shown that variations of the temperature and solar radiation have the strongest effect on the emission of isoprene and other volatile compounds. The measurements of emissions from 34 pine species in California[65] showed that pine trees emitted only when illuminated and the emission increased exponentially up to the temperature of 35°C. Above 42°C the emission rate decreased fast.

Consequently, the increase in the UV radiation influx with the increasing solar activity leads to the growth of the temperature and emission of volatile organic compounds, if the UV radiation dose does not exceed the destructive level for a given plant species.

However, in the period of intensification of photochemical processes due to increase in the UV-B radiation and in the emission of ozone-forming substances into the atmosphere, toxic compounds are produced in air, and they inhibit plants, that is, a feedback arises. According to Ref. 66, the increase of the ozone concentration above the level of 30 μg/m^3 can result in up to 50% loss in the plant productivity. Semenov with co-authors has calculated the harvest loss for Europe due to the increased ozone content.[67] It turned out that in the period from 1991 to 1994 this value, on the average, was 6–17% depending on the country. The emission of volatile compounds should likely change by the same value. In spite of the decrease in the plant productivity, near-surface ozone causes an injury of leaves, as well as leads to some shifts in competitive advantages of individual plant species in mixed populations.[19]

Summarizing this analysis, we can conclude that there are real prerequisites for revealing the mechanism of signal transmission from the Sun to the Earth, which possibly is realized through the tropospheric air composition.

Initial materials

For investigations, we used the data of aerosol measurements onboard the instrumented aircrafts Il-14 and An-30 Optik-E, as well as at the ground-based TOR station. The NOAA and NASA satellite results and, if necessary, synoptic maps were also involved.

In addition to statistical data processing methods, we used the superposed epoch method, which is commonly used when studying solar–terrestrial relations.[2–5] In this section we briefly characterize the materials used.

The description of the instrumented aircrafts Il-14 and An-30 Optik-E can be found in Refs. 68 and 69. An AZ-5 photoelectric particle counter with the specially developed parallel analyzer was used to measure the aerosol number density. The counter measures the number of particles with the size from 0.4 to 10 μm in the unit volume in 12 channels divided by the log scale. The measurement error did not exceed 20%. Since the counter often got out of order under the severe onboard operating condition (vibration, temperature differences from −40 to +40°C, etc.), to make the results comparable, in the ground-based laboratory we had the reference device used to calibrate the repaired counter.

Under processing were vertical profiles of the aerosol ($d \ge 0.4$ μm) number density measured at the aircraft take-off or landing in different airports of Western Siberia in the period from 1984 to 1991, when the aircraft laboratories operated in the quasi-monitoring mode. A total of 5 000 of vertical profiles were involved. The cases that the airport was under the effect of the nearest city were preliminarily excluded from the sample. We used only the mean aerosol number density in the lower 3-km atmospheric layer rather than the whole profile:

$$\overline{N} = \frac{1}{H}\int_0^H N(h)\,\mathrm{d}h$$

Here h is the height; N is the aerosol number density, in cm^{-1}.

In the early 1990s the airborne program of the IAO SB RAS was suspended by economical reasons. Therefore, starting from December of 1992, ground-based measurements were organized in the region of Tomsk Akademgorodok. The created automatic station was called TOR station in accordance with the EEC Tropospheric Ozone Research Project. The description of the TOR station latest version can be found in Ref. 70. Ozone at the TOR station is measured with the domestic O3-2P ozonometer of 1–1000 μg/m^3 range at the error of 12%. The aerosol number density is measured by the same AZ-5 aerosol counter as in the instrumented aircrafts.

The TOR station is located at a three-storied building on the north-eastern periphery of Tomsk Akademgorodok in the forest. There are no industrial objects and highways near the building. Measurements at the station are conducted 24 hours all-the-year-round with the interval of 1 h. The time of one measurement is 10 min, and during this time 600 readings are obtained and averaged. Since the station employs the equipment based on the contact aspiration method, the aspiration of all sampling devices starts 10 min before the start of measurements to purge all communications. To reveal possible anthropogenic effects from neighboring Tomsk city, specialized experiments were conducted. For this purpose, two similar stations were operating synchronously in the background region (Kireevsk, Tomsk Region) and in Akademgorodok. It was found that the anthropogenic effect, if any, manifests itself in no more than 10% of cases and does not exceed 30% in the absolute value for most parameters, including aerosol.

Table 3

Year	1993	1994	1995	1996	1997	1998	1999	2000	2001	Total
Number of measurements	7980	8342	8165	7989	8224	8347	8241	8097	8169	73554

In this work we used the annual mean data on the aerosol number density ($d \geq 0.4$ μm) and the near-surface ozone concentration. The quantity of the hourly measurements used is given in Table 3. The cases with the pronounced anthropogenic effect were excluded from our analysis.

To compare the measurements in Tomsk with the general regional situation, we used the satellite results for the area of 85°–87°E and 55°–57°N available in the Internet: Ref. 71 for UV radiation and Ref. 72 for the total ozone content. The data on the Wolf numbers and the solar radio emission at $\lambda = 10.7$ cm were also received from the Internet.[73]

Sometimes debates arise concerning the solar characteristic to be used in analysis of the solar-terrestrial relations: the Wolf number or the emission at $\lambda = 10.7$ cm. The comparison of these parameters in Fig. 2 shows that this problem is not of principal importance when considering the annual mean characteristics.

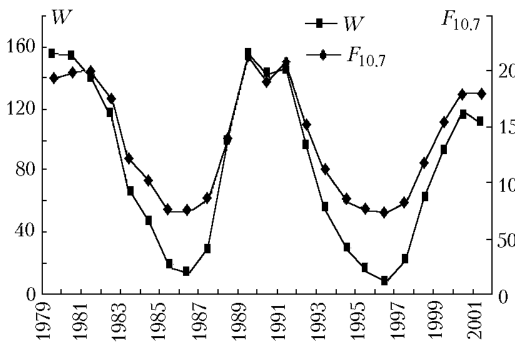

Fig. 2. Annual mean Wolf number and radiation at $\lambda = 10.7$ cm.

For combined investigation of plant's state, we used the so-called normalized difference vegetation index (NDVI), the data on which are also available in the Internet.[74]

This characteristic is still uncommon in the scientific literature relating to our subject, therefore, we explain it in more detail.

To obtain the vegetation index, the first and second NOAA AVHRR channels are used. The first channel (0.58–0.68 μm) gives the information about solar radiation absorption by plant chlorophyll. The second channel receives the reflected radiation in the range 0.78–0.90 μm. Then the index is calculated as

$$\text{NDVI} = \frac{J_{\lambda 1} - J_{\lambda 2}}{J_{\lambda 1} + J_{\lambda 2}},$$

where $J_{\lambda 1}$ and $J_{\lambda 2}$ are, respectively, the signals in the first and second AVHRR channels.

According to Ref. 75, the normalized difference vegetation index is strongly correlated with the vegetation parameters, such as the green biomass and green vegetation regions. The application of this index to analysis of the CO_2 dynamics in Ref. 76 gave very good results.

Shishkin[77] noted that NDVI depends on the growth and development of tree crowns and well reflects their dynamics. It was also noted that NDVI represents actual observations over the absorbed active photosynthetic radiation, which is an indicator of potential photosynthesis determining the productivity of trees. The real values of photosynthesis and productivity depend not only on the physical property of an ecosystem to absorb the solar energy, but also on other characteristics, such as watering, state of the soil, etc. Therefore, the real photosynthesis is always lower than that measured by NDVI.

In our investigation, NDVI is considered as a combined plant characteristic, which reflects possible emissions of volatile compounds – ozone-forming gases – by trees.

Many-year variations of ozone and aerosol concentration in Tomsk and their possible causes

Measurement of the aerosol number density, first, onboard the instrumented aircraft over the territory of Western Siberia and then the ground-based measurements of the aerosol number density and the ozone concentration near Tomsk revealed that both these air constituents experience many-year variability with the period close to 11 years. Variations of the aerosol number density and the ozone concentration are shown in Fig. 3.

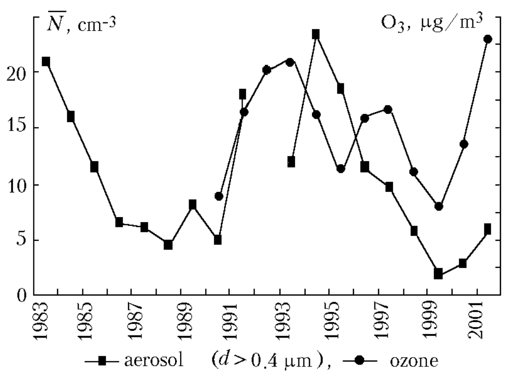

Fig. 3. Annual mean values of the aerosol number density and the surface ozone concentration near Tomsk.

It is seen that in the period from 1983 to 1988 the aerosol number density decreased, and in 1990 it began to grow. Then we had a break in measurements. The next period of the aerosol number density decrease started in 1994 (just 11 years later) and ended in 1999, and then it began to increase again. Thus, for almost 20 years we observed two many-year cycles of decrease and increase of the aerosol concentration. In the 1980s the aerosol number density changed 5-fold, while in the 1990s it changed almost 20-fold, what many times exceeds possible measurement errors.

The ozone concentration has been measured for 11 year. It also demonstrates the many-year behavior similar to that of aerosol. The only exclusion is 1995. The cause for the ozone decrease that year is still unknown.

It is also seen in Fig. 3 that first the ozone concentration began to decrease in the 1990s, and then the aerosol number density followed it. From 1993 to 1995 the lag was equal to 1 year. In 1995–1997 the lag with respect to ozone became inverted, but also equal to 1 year. Staring from 1999 the aerosol number density and ozone increased synchronously. It should be noted that the growth of the aerosol number density was predicted by us.[78]

Such large-amplitude variations of ozone and aerosol can cause some doubts. Therefore, it is worth comparing our results with other data.

From the balloon-borne measurements of the aerosol number density in USA in 1983–1989, Hofmann revealed its almost tenfold decrease in the 5–10 km layer and roughly threefold decrease in the 2–5 km layer.[79] These results in both time and magnitude are close to our data presented above. The concentration of sulfates, nitrates, and ammonium in aerosol particles has been studied from 1990 to 1995 in Northeast Greenland.[80] First, the increase of the concentration with the maximum in 1993 was found, and then the concentration decreased 1.5–2 times. Analysis of the aerosol optical depth for the period from 1980 to 1996 in Poland showed[81] that it decreased slowly by ~ 7.4% a year at the same periods as in Refs. 79 and 80, but then fast recovered in the period of growth. Abakumova in Moscow[82] has obtained the pattern for the aerosol depth similar to Fig. 3.

The trends of the ozone concentration close in time to that shown in Fig. 3 were obtained for Kislovodsk,[83] Greece,[84] Finland,[85] and Denmark.[86] It should be noted that the results[84–86] were obtained for regions burdened by the anthropogenic impact, and the dynamics there is not so pronounced as in Fig. 3 and in Ref. 83.

Besides the aerosol and ozone trends, some investigators observed many-year variations in the concentration of the ozone- and aerosol-forming gases: NO_x and CO in the region of the Mexico City,[87] NO_x, ethane, acetylene, and propen in Norway.[88]

Consequently, the many-year aerosol and ozone variations shown in Fig. 3 are of non-random and non-regional character. Moreover, they reflect some regularities having, at least, the hemispherical character.

In Ref. 89 we analyzed the causes of variation of the aerosol number density in the first cycle (1980s). We have considered and rejected the hypotheses about the anthropogenic and postvolcanic (El Chichon, Mt. Pinatubo) origin of the trend. The variation of the aerosol number density turned out to correlate best with the Kats's *W*, *E*, and *C* forms, which are determined, as known, by the solar activity.[90]

Thus, the 11-year periodicity and the preliminary analysis allow us to pass on to the search of causes for these trends in different characteristics of the solar activity.

Relation of many-year ozone and aerosol variations with the solar activity

Consider first the mutual many-year behavior of the aerosol number density (Fig. 4) and solar activity represented by the radio emission of the entire Sun's surface at λ = 10.7 cm, as well as ozone and the solar activity (Fig. 5).

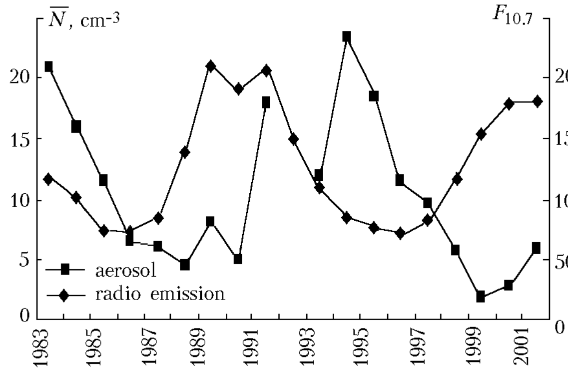

Fig. 4. Annual mean values of radio emission $F_{10.7}$ and the aerosol number density near Tomsk.

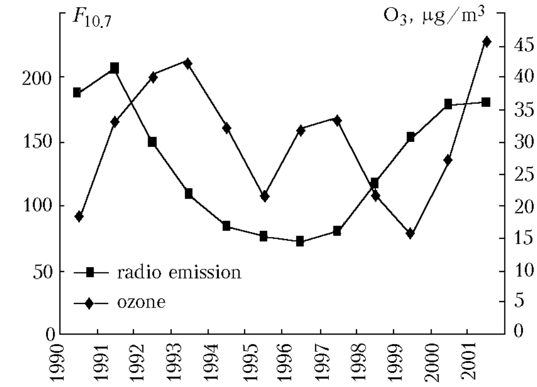

Fig. 5. Annual mean values of radio emission $F_{10.7}$ and the surface ozone concentration near Tomsk.

It is seen in Fig. 4 that the aerosol number density follows the behavior of the solar activity for the last two 11-year cycles with the lag of 2 years in the first cycle and 3 years in the second cycle. The different values of the lag are possibly caused by the fact that, in addition to the 11-year cycle, the Sun has the 22-year cycle joining neighboring cycles, that is, the so-called cycle parity.[91]

The parity of the solar activity cycle is connected with the global reconstruction of the Sun's global magnetic field. The even and odd cycles are characterized by different signs of the global (poloidal) magnetic field in the Sun's polar regions and alternation of the field sign of leading sunspots in the groups of the given hemisphere. The character of interaction of the Sun's and Earth's atmospheres changes correspondingly. Reference 91 just describes the 1-year shift between the even and odd cycles.

It is possible to compare the behavior of the ozone concentration and the solar activity during one 11-year cycle (see Fig. 5). Here we can also see the lag, on the average, of 3 years. The increase in the surface ozone concentration, begun in 2000, after the increase in the solar radio emission has a shorter lag, that is, 2 years.

Thus, we can see from Figs. 4 and 5 that the both components: ozone and aerosol, copy the behavior of the solar activity with the lag of 2–3 years.

We have also compared the behavior of TOC and the solar activity, but failed to find some regularity or anticorrelation. At the same time, the comparison of the many-year TOC variability and the behavior of the surface ozone concentration (SOC) shown in Fig. 6 gave a positive result.

It is seen from Fig. 6 that for the most part of the 11-year cycle these characteristics are in antiphase. When the total ozone content decreases, the surface ozone concentration increases, and vice versa. The exceptions are only 1990 and 1995.

The data of Fig. 6 allow us to come back to the above-mentioned ozone mechanism of signal transmission from the Sun to the Earth.[6]

If the decrease in TOC leads to the increase in the UV radiation influx to the lower troposphere, then this should be reflected in the rate of the surface ozone generation.

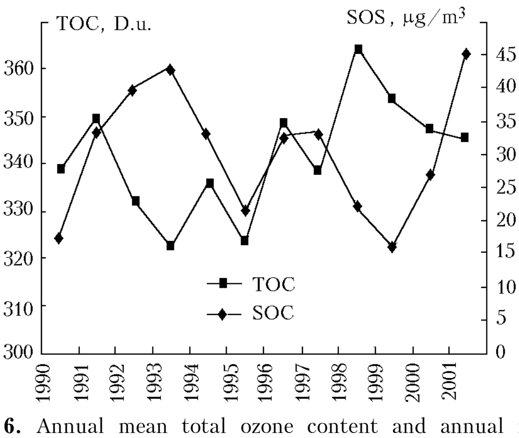

Fig. 6. Annual mean total ozone content and annual mean surface ozone concentration near Tomsk.

Figure 7 shows that in the period of the solar activity growth (1988–1990) the UV radiation influx increases as well. However, the surface ozone concentration begins to increase only 2 years later the beginning of this process.

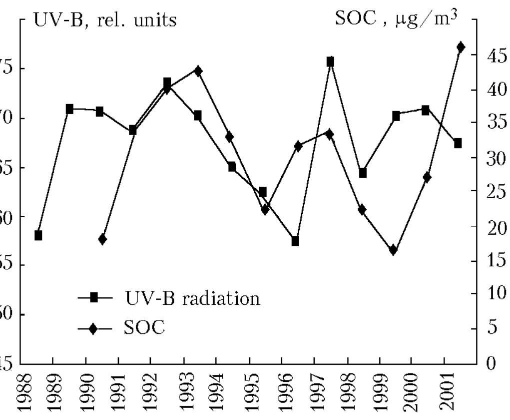

Fig. 7. Annual mean UV-B radiation flux and the annual mean surface ozone concentration near Tomsk.

Then (in 1991–1995) the surface ozone varied almost synchronously with the tendency of UV radiation variation. It should be noted that the satellite data have a gap in 1994–1996, which is filled with the results of Ref. 92. To all appearances, some oscillation process occurred in the atmosphere in the period of 1995–1996. In 1997 the solar activity began to increase in the next cycle, and this was reflected in the UV radiation influx. However, the growth of the surface ozone concentration started only in 2000, that is, again 2 years later, as in the beginning of the previous cycle. This suggests that in the many-year relation of the UV radiation and surface ozone there are some differences in the ascending and descending branches. Thus, the growth of UV radiation on the ascending branch is ahead of the surface ozone concentration, and on the descending branch they vary almost synchronously.

The similar relation can be found between aerosol and the UV radiation during the most part of the 22-year cycle (Fig. 8).

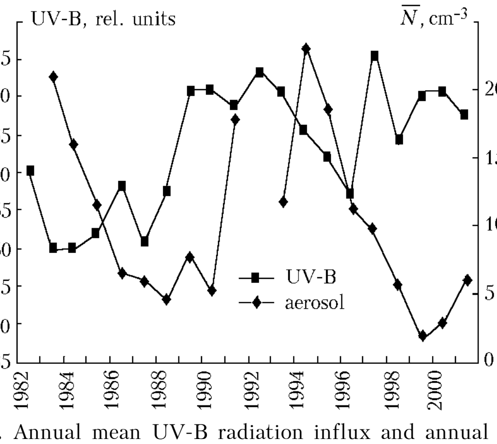

Fig. 8. Annual mean UV-B radiation influx and annual mean aerosol number density near Tomsk.

It is seen from Fig. 8 that there is a lag between the UV radiation influx variation and the behavior of the aerosol number density from 1983 to 1996. Then this lag was disturbed and reconstructed again since 1998.

Thus, it turns out that some intermediate mechanism introducing the lag exists between the UV radiation influx and the increase or decrease of ozone and aerosol. In our opinion, this mechanism is the interaction between the UV radiation and plants.

Possible role of plants in delay of ozone and aerosol generation

To consider how plants can affect ozone and aerosol generation, we estimate the balance of substances taking part in photochemical processes.

Write the gross equation of surface ozone generation as[93]:

$$\mathrm{RH} + \mathrm{CO} + \mathrm{NO} \xrightarrow{h\nu, O_2, H_2O} \mathrm{NO_2} + f\,\mathrm{H_2CO} + k\mathrm{O_3} + P,$$

where f and k are the stoichiometric conversion coefficients of hydrocarbons RH; P are reaction products, usually, microdispersion aerosol particles.

It follows from this equation that the reaction yield depends not only on the UV influx $h\nu$, but also on the input amount of the substance, that is, on the concentration of hydrocarbons RH, carbon oxide, and nitrogen oxides in air. The data available in the global monitoring system[94] show no significant changes of CO and NO in different regions. A network for RH monitoring does not exist yet. Therefore, variation of just this characteristic is most probable. Recall that hydrocarbons come to the atmosphere mostly with plant emissions.

The mechanism of delay seems to be the following. The increase of the UV influx in the period of growth of the solar activity has an inhibiting effect on plants. An adaptation period of 2–3 years is needed. Then, having adapted to the increased UV background, plants begin to emit extra amounts of volatile organic compounds. This, judging from the above gross equation, must result in maximal concentration of both ozone and fine aerosol, what is well confirmed by the results of Ref. 95.

How can we check this hypothesis without RH measurements? For this purpose, let us look at the vegetation index, which should reflect the general state of plants, along with their productivity.

It is seen from Fig. 9 that the surface ozone concentration almost fully copies the behavior of the vegetation index for the region of measurements. Certainly, this result does not prove completely the above hypothesis, but it allows us to explain the relation between the air composition and solar activity.

The same pattern is observed for aerosol, as can be seen from Fig. 10. However, there is a difference between the 21st and 22nd 11-year cycles. In the 1980s the decrease of NDVI and aerosol was synchronous, but not so large as in the 1990s. It is worth recalling that the concentration decrease in the 1980s was also smaller than in the 1990s.

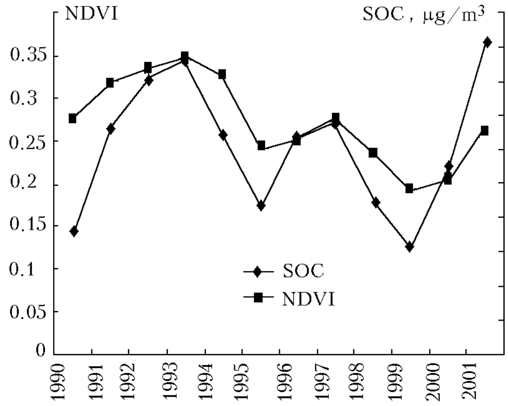

Fig. 9. Annual mean NDVI and the annual mean surface ozone concentration near Tomsk.

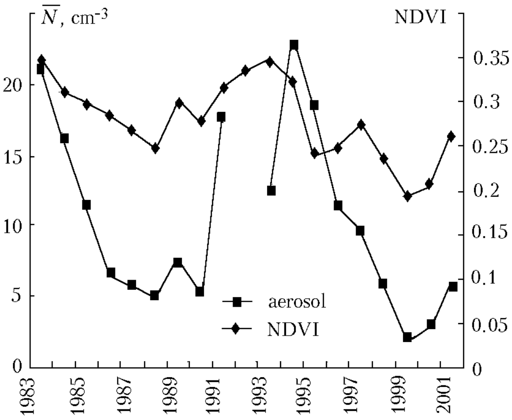

Fig. 10. Annual mean values of NDVI and annual mean aerosol number density near Tomsk.

It can be argued, that the plant productivity depends not only on the UV influx, but also on the climatic (temperature, humidity) and geophysical (soil) factors. But many of these factors also positively correlate with the solar activity.[96–101] What is more, still in Ref. 3 Chizhevskii obtained a shift of 2–3 years between the maximum solar activity and the air temperature in different regions.

Prediction of variation of ozone and aerosol concentration in 2003–2008

Rather stable in time characteristics of solar activity allow us to predict its behavior with a certain degree of accuracy, as was done in Refs. 2–4 and 102–104.

According to Refs. 103 and 104, the maximum of the 23rd cycle began in 2001 and lasted up to the beginning of 2002, and the minimum is expected in 2007–2008. Taking into account the parity of the cycles, its intensity should be somewhat lower than that of the previous 22nd cycle and equal to 60 ± 20 in the Wolf numbers.

Based on this information and taking into account the lag between the solar activity, we can find the reference points in the ozone and aerosol concentrations (Table 4).

Table 4

Parameter	Maximum period	Minimum period	Maximum value	Minimum value
Aerosol	2004	2008	(22±4) cm^{-3}	(4±1) cm^{-3}
Ozone	2003	2008	(55±6) $\mu g/m^3$	(15±2) $\mu g/m^3$

Measurements in the previous cycles show that the maximal values in the 11-year cycles are roughly the same and determined, most probably, by the plant productivity in a given region. The minimal value depends on the intensity of UV influx variation, and, with allowance for the cycle parity, the next cycle should be characterized by a smaller decrease. In the periods between 2003 and 2008, we can suppose a linear variation of the ozone and aerosol concentration.

Conclusion

During investigations, it was found that atmospheric constituents of photochemical origin vary with the 11-year periodicity, and these variations are not synchronous. The ozone and aerosol concentrations in their behavior have a lag of 2–3 years with respect to changes of solar activity.

In search of the causes for such a behavior, we analyzed sequentially the ozone mechanism and the consequences of UV influx variations and came to some intermediate mechanism. Hypothetically, this mechanism is caused by interaction between the increasing UV radiation and plants. At the beginning of the process, the increasing UV radiation inhibits plants, then, after the 1–2-year adaptation period their productivity increases, what results in the extra emission of ozone- and aerosol-forming substances into the atmosphere. This hypothesis was checked using the normalized difference vegetation index and gave good results. The mechanism proposed is also confirmed by the results of Refs. 105–107, which indicate that plants have so-called long-term cumulative effect at intensification of the UV-B radiation. This effect consists in delay of plant photosynthesis by 2–3 years with respect to the UV-B irradiation arrival.

References

1. Ch.A. Young, *The Sun* (1881).
2. V.F. Chistyakov, Izv. TNIRTs **122**, 40–71 (1997).
3. A.L. Chizhevskii, *Terrestrial Echo of Solar Storms* (Mysl', Moscow, 1976), 367 pp.
4. B.M. Vladimirskii, Biofizika **43**, No. 4, 566–570 (1998).
5. B.M. Vladimirskii and N.A. Temur'yants, *Effect of the Solar Activity on the Biosphere–Noosphere* (MNEPU, Moscow, 2000), 374 pp.
6. K.Ya. Kondratyev and G.A. Nikol'skii, Issled. Zemli iz Kosmosa, No. 5, 3–17 (1995).
7. K.Ya. Kondratyev and G.A. Nikol'skii, Issled. Zemli iz Kosmosa, No. 6, 3–17 (1995).
8. M.S. Eigenson, M.N. Gnevyshev, A.I. Ol', and B.M. Rubashev, *Solar Activity and Its Terrestrial Manifestations* (Gostekhizdat, Moscow, Leningrad, 1948), 323 pp.
9. Yu.I. Vitinskii, A.I. Ol', and B.I. Sazanov, *The Sun and the Earth's Atmosphere* (Gidrometeoizdat, Leningrad, 1976), 351 pp.
10. V.F. Loginov, Tr. VNIIGMI-MTsD, Issue 23, 6–29 (1975).
11. E.V. Kononovich and N.N. Shefov, Dokl. Ros. Akad. Nauk **367**, No. 1, 108–111 (1999).
12. G.A. Nikol'skii and E.O. Shul'ts, Problems of Atmospheric Physics, Issue 20, 232–241 (1995).
13. B.A. Tinsley and G.W. Deen, J. Geophys. Res. D **96**, No. 9, 22283–22296 (1991).
14. S.V. Veretenenko and M.I. Pudovkin, Geomagn. Aeron. **38**, No. 5, 33–42 (1998).
15. G.S. Ivanov-Kholodnyi, Zemlya i Vselennaya, No. 2, 80–86 (1998).
16. P.G. Crutzen, I.S.A. Isaksen, and G.C. Reid, Science **189**, 457–459 (1975).
17. A.A. Krivolutskii, A.A. Kuminov, and A.I. Repnev, Geomagn. Aeron. **39**, No. 3, 3–15 (1999).
18. C.A. Varotsos and K.Ya. Kondratyev, Issled. Zemli iz Kosmosa, No. 4, 3–13 (1998).
19. G.I. Marchuk, K.Ya. Kondratyev, A.E. Aloyan, and C.A. Varotsos, Issled. Zemli iz Kosmosa, No. 5, 12–30 (1999).
20. V.K. Roldugin, Meteorol. Gidrol., No. 10, 53–58 (2000).
21. S.P. Perov and A.Kh. Khrgian, *Current Problems of Atmospheric Ozone* (Gidrometeoizdat, Leningrad, 1980), 288 pp.
22. E.M. Volodin and V.Ya. Galin, Dokl. Ros. Akad. Nauk **362**, No. 4, 544–547 (1998).
23. P.J. Michaels, S.F. Singer, O.P.E. Knapperberger, et al., Science **264**, 1527–1547 (1994).
24. U. Feister and R. Grewe, Glob. Planet. Change **11**, No. 1, 25–34 (1995).
25. J.E. Frederick, Qu Zheng, and C.R. Booth, Photochem. Photobiol. **68**, No. 2, 183–190 (1998).
26. C. Zerefos, C. Meleti, and D. Balis, Geophys. Res. Lett. **25**, No. 23, 4345–4348 (1998).
27. R.L. Me Kenzie, World Clim. Res. Programme, World. Meteorol. Organ. **2**, No. 814, 517–520 (1997).
28. C.A. Varotsos, G.J. Chronopoulos, A.P. Cracknell, et al., Int. J. Remote Sens. **19**, No. 17, 3301–3305 (1998).
29. K.R. Gurney, Geophys. Res. Lett. **25**, No. 6, 903–906 (1998).
30. H. Piazena, Solar Energy **57**, 133–140 (1996).
31. M. Blumithaler, in: *Environ. Effects of UV Radiation* (Lewis Publ., Boca Raton, 1993), pp. 17–69.
32. S. Cabrera, S. Bozzo, and H. Fuenzalida, Photochem. Photobiol. **28**, No. 2, 137–142 (1995).
33. V.E. Fioletov, E. Griffieen, J.B. Kerr, et al., Geophys. Res. Lett. **25**, No. 10, 1655–1658 (1998).
34. V.A. Belinskii, M.P. Garadzha, L.M. Mezhennaya, and E.I. Nezval', *Celestial and Solar UV Radiation* (Publishing House of Moscow State University, Moscow, 1968), 228 pp.
35. N.P. Rusin, *Applied Actinometry* (Gidrometeoizdat, Leningrad, 1979), 232 pp.
36. G.M. Kruchenitskii, A.M. Zvyagintsev, N.S. Ivanova, and I.N. Kuznetsova, Meteorol. Gidrol., No. 11, 113–120 (2000).
37. R.C. Willson, The Earth Observer **7**, No. 1, 39–48 (1995).
38. D. Crommelynck, Issled. Zemli iz Kosmosa, No. 5, 18–21 (1995).
39. Yu.A. Sklyarov, Issled. Zemli iz Kosmosa, No. 4, 96–110 (1994).
40. Yu.A. Sklyarov, V.A. Dvinskikh, Yu.I. Brichkov, and A.I. Kotuma, Issled. Zemli iz Kosmosa, No. 6, 40–46 (1998).
41. V.A. Isidorov, *Ecological Chemistry* (Khimizdat, St. Petersburg, 2001), 304 pp.
42. P.J. Crutzen, in: *Remote Sens. and Earth's Environ.* (1990), pp. 105–113.
43. D.H. Enhalt, Sci. Total Environ. **143**, No. 1, 1–15 (1994).
44. A.P. Mitra, Indian J. Radio and Space Phys. **19**, Nos. 5–6, 383–399 (1990).

45. E.L. Aleksandrov, I.L. Karol', L.R. Rakipova, et al., *Atmospheric Ozone and Global Climate Changes* (Gidrometeoizdat, Leningrad, 1982), 168 pp.
46. A.A. Kiselev and I.L. Karol', Meteorol. Gidrol., No. 7, 12–22 (2001).
47. J. Landgraf and H.J. Crutzen, J. Atmos. Sci. **55**, No. 3, 863–878 (1998).
48. B.D. Belan, V.V. Zuev, T.K. Sklyadneva, S.V. Smirnov, and G.N. Tolmachev, Atmos. Oceanic Opt. **13**, No. 10, 860–864 (2000).
49. B.C. Kruger, A. Martilli, and J. Kubler, Ann. Geophys. **15**, No. 3, 701 (1997).
50. Kraus and A. Hofzumahaus, J. Atmos. Chem. **31**, Nos. 1–2, 161–188 (1998).
51. Ma Jianzhong and R. Guicherit, Photochem. Photobiol. **66**, No. 3, 346–355 (1997).
52. V.A. Isidorov, *Organic Chemistry of the Atmosphere* (Khimizdat, St. Petersburg, 2001), 352 pp.
53. V.G. Gorsikov and A.M. Makar'eva, Issled. Zemli iz Kosmosa, No. 5, 3–11 (1999).
54. V.G. Gorshkov and K.Ya. Kondratyev, Ekologiya, No. 1, 7–16 (1990).
55. I.A. Shul'gin, *Solar Radiation and Plant* (Gidrometeoizdat, Leningrad, 1967), 180 pp.
56. G.V. Dobrovol'skii and E.D. Nikitin, *Soil Functions in Biosphere and Ecosystems (Ecological Concern of Soil)* (Nauka, Moscow, 1990), 261 pp.
57. G.V. Dobrovol'skii, *Principles of Biogeochemistry* (Vyssh. Shkola, Moscow, 1998), 413 pp.
58. D. Ort, B.A. Melandri, B. Younge, et al., *Photosynthesis* (Mir, Moscow, 1987), Vol. 7, 460 pp.
59. E.A. Kamenir and A.K. Kirillov, Biofizika **43**, No. 5, 920–925 (1998).
60. G.F. Plekhanov, *Living Systems in Electromagnetic Fields* (TGU Publ., Tomsk, 1978), 308 pp.
61. K.A. Samoilova, *Effect of Radiation on a Cell* (Nauka, Moscow, 1967), 146 pp.
62. V.A. Isidorov, *Volatile Plant Egesta: Composition, Emission Rate, and Ecological Role* (Alga, St. Petersburg, 1994), 188 pp.
63. M. Owen Susan, C. Boissard, B. Hagenlocher, and C. Nidalas Hewitt, J. Geophys. Res. D **103**, No. 19, 25499–25511 (1998).
64. R. Janson and C. De Serves, J. Geophys. Res. D **103**, No. 19, 25513–25517 (1998).
65. P. Harley, V. Fridd-Stroud, J. Greenberg, et al., J. Geophys. Res. D **103**, No. 19, 25479–25486 (1998).
66. W.H. Smith, *Air Pollution and Forests* (Springer-Verlag, New York, 1981), 430 pp.
67. S.M. Semenov, I.M. Kunina, and B.A. Kukhta, *Meteorology and Hydrology* (Moscow, 1999), 208 pp.
68. B.D. Belan, in: *Instrumentation for Remote Sensing of Atmospheric Parameters* (TA SB AS USSR, Tomsk, 1987), pp. 34–40.
69. V.E. Zuev, B.D. Belan, D.M. Kabanov, V.K. Kovalevskii, O.Yu. Luk'yanov, V.E. Meleshkin, M.K. Mikushev, M.V. Panchenko, I.E. Penner, E.V. Pokrovskii, S.M. Sakerin, S.A. Terpugova, G.N. Tolmachev, A.G. Tumakov, V.S. Shamanaev, and A.I. Sherbatov, Atmos. Oceanic Opt. **5**, No. 10, 658–663 (1992).
70. M.Yu. Arshinov, B.D. Belan, D.K. Davydov, et al., Meteorol. Gidrol., No. 3, 110–118 (1999).
71. ftp://toms.gsfe.nasa.gov/pub/eptoms/data/montly averages/uv/
72. ftp://toms.gsfe.nasa.gov/pub/eptoms/data/montly averages/ozone
73. http://spidr.ngdc.noaa.gov/index.html
74. http://www.saa.noaa.gov/swwig-lin/wwwdisplay
75. C.O. Justice, J.R.G. Townshend, B.N. Holben, and C.J. Tucker, Int. J. Remote Sens., No. 6, 1271–1318 (1985).
76. M.Ya. Antonovskii, V.M. Bukhshtaber, and V.A. Pivovarov, Meteorol. Gidrol., No. 2, 16–24 (2002).
77. E.A. Shishkin, "*Systematic analysis of spatiotemporal dynamics of primary productivity indices of trees in Siberia*," Author's Abstract of Cand. Tekh. Sci. Dissert., Krasnoyarsk (2002), 21 pp.
78. M.Yu. Arshinov, B.D. Belan, V.K. Kovalevskii, A.P. Plotnikov, T.K. Sklyadneva, and G.N. Tolmachev, Atmos. Oceanic Opt. **13**, Nos. 6–7, 580–583 (2000).
79. D.J. Hofmann, J. Geophys. Res. D **98**, No. 7, 12753–12766 (1993).
80. N.Z. Heidam, P. Wahlin, and J.H. Christensen, J. Atmos. Sci. **56**, No. 1, 261–278 (1999).
81. J.W. Krzyscin and S. Puchalski, J. Geophys. Res. D **109**, No. 13, 16175–16181 (1998).
82. G.M. Abakumova, Meteorol. Gidrol., No. 9, 51–62 (2000).
83. N.F. Elansky, A.Ya. Arabov, I.A. Senik, et al., in: *EUROTRAC: TOR-2 Annual Report-2000* (GSF, Munich, 2001), pp. 72–75.
84. T. Butkovic, T. Cvitas, K. Dzepina, et al., *Ibid*., pp. 89–92.
85. T. Laurila, H. Hacola, V. Lindfors, and J.-P. Tuoviken, *Ibid*., pp. 93–97.
86. H. Skov, A.H. Egelov, K. Kemp, et al., *Ibid*., pp. 127–130.
87. L.T. Molina and M.J. Molina, EUROTRAC Newsletter, No. 23, 4–9 (2001).
88. M. Roster, *TNO Report R 2001/100* (Apeldoorn, 2001), 55 pp.
89. V.G. Arshinova, B.D. Belan, E.V. Vorontsova, G.O. Zadde, T.M. Rasskazchikova, O.I. Sem'yanova, T.K. Sklyadneva, and G.N. Tolmachev, Atmos. Oceanic Opt. **10**, No. 8, 577–582 (1997).
90. L.A. Vitel's, *Synoptic Meteorology and Heliogeophysics* (Gidrometeoizdat, Leningrad, 1977), 256 pp.
91. I.F. Nikulin, Biofizika **43**, No. 5, 900–901 (1998).
92. M.V. Vinarskii, I.I. Ippolitov, and M.V. Kabanov, Atmos. Oceanic Opt. **15**, No. 4, 363–364 (2002).
93. B.D. Belan, Atmos. Oceanic Opt. 9, No. 9, 754–773 (1996).
94. http://www.cmdl.noaa.gov/ccgg/globalview/
95. M.Yu. Arshinov and B.D. Belan, Atmos. Oceanic Opt. **13**, No. 11, 909–916 (2000).
96. A.N. Fakhrutdinova, Yu.P. Perevezentsev, and D.V. Korotyshkin, in: *Proc. Research Conf. Devoted to 10th Anniversary of MSG* (Gidrometeoizdat, St. Petersburg, 2002), pp. 53–55.
97. O.M. Raspopov, N.V. Lovelius, O.I. Shumilov, and E.A. Kasatkin, Biofizika **43**, No. 5, 863–867 (1998).
98. M. Tomasino and F. Dalla Valle, Hydrol. Sci. J. – J. des Sci. Hydrol. **45**, No. 6, 477–490 (2000).
99. J. Hansen, M. Sato, J. Glascoe, R. Ruedy, Proc. Nat. Acad. Sci. USA **95**, No. 8, 4113–4120 (1998).
100. R.V. Smirnov, Biofizika **43**, No. 4, 689–693 (1998).
101. S.K. Solanki and M. Fligge, Geophys. Res. Lett. **25**, No. 3, 341–344 (1998).
102. A.K. Pankratov, V.Ya. Narmanskii, and V.M. Vladimirskii, Biofizika **43**, No. 5, 888–891 (1998).
103. A.K. Pankratov, V.Ya. Narmanskii, and V.M. Vladimirskii, Biofizika **43**, No. 5, 883–887 (1998).
104. K. Schatten and D. Hoyt, Geophys. Res. Lett. **25**, No. 5, 599–601 (1998).
105. J.H. Sullivan and A.H. Teramura, Plant Physiologie **92**, No. 2, 141–146 (1990).
106. J.H. Sullivan and A.H. Teramura, Trees **6**, No. 1, 115–120 (1992).
107. A.H. Teramura and J.H. Sullivan, Photosynthesis Res. **39**, No. 3, 463–473 (1994).